Bioorganic & Medicinal Chemistry 19 (2011) 6302–6308

Contents lists available at SciVerse ScienceDirect

Bioorganic & Medicinal Chemistry

journal homepage: www.elsevier.com/locate/bmc

Identification of new antimalarial leads by use of virtual screening against cytochrome bc_1

Tiago Rodrigues [a], Rui Moreira [a,*], Jiri Gut [b], Philip J. Rosenthal [b], Paul M. O'Neill [c], Giancarlo A. Biagini [d], Francisca Lopes [a], Daniel J.V.A. dos Santos [a], Rita C. Guedes [a]

[a] Research Institute for Medicines and Pharmaceutical Sciences (iMed.UL), Faculty of Pharmacy, University of Lisbon, Av. Prof. Gama Pinto, 1649-019 Lisbon, Portugal
[b] Department of Medicine, San Francisco General Hospital, University of California, San Francisco, Box 0811, San Francisco, CA 94143, USA
[c] Department of Chemistry, University of Liverpool, Crown Street, Liverpool L69 7ZD, United Kingdom
[d] Molecular and Biochemical Parasitology, Liverpool School of Tropical Medicine, University of Liverpool, Liverpool L3 5QA, United Kingdom

ARTICLE INFO

Article history:
Received 4 July 2011
Revised 31 August 2011
Accepted 5 September 2011
Available online 10 September 2011

Keywords:
Malaria
Virtual screening
Cytochrome bc_1
Pharmacophore

ABSTRACT

Cytochrome bc_1 is a validated drug target in malaria parasites. The spread of *Plasmodium falciparum* strains resistant to multiple antimalarials emphasizes the urgent need for new drugs. We screened in silico the ZINC and MOE databases, using ligand- and structure-based approaches, to identify new leads for development. The most active compound presented an IC_{50} value against cultured *P. falciparum* of 2 μM and a docking pose consistent with its activity.

1. Introduction

Malaria remains the most important vector-borne infectious disease in the world and is responsible for approximately 1 million deaths each year.[1] The spread of multidrug-resistant *Plasmodium falciparum* strains has renewed interest in finding novel drugs for both treatment and prophylaxis of malaria. The mitochondrial electron transport-chain has proved to be a valid chemotherapeutic target because of significant differences between plasmodial and analogous mammalian enzymes.[2,3] Atovaquone, **1**, was introduced in the late 1990s, in combination with proguanil, to treat and prevent multidrug-resistant malaria.[4,5] Cytochrome bc_1 is the primary target of atovaquone.[6] Recently it was proposed that atovaquone binds to the oxidation site (Q_o) of cytochrome *b* and to the iron–sulfur protein (ISP) subunit,[7,8] displacing ubiquinol and blocking the required conformational shift of the ISP to transfer electrons, thus shutting down pyrimidine biosynthesis and leading to parasite death.[4] Despite the effectiveness of atovaquone, resistance swiftly emerged.[9] Interest in developing novel inhibitors of the bc_1 complex led to the re-discovery of the anticoccidial drug clopidol, **2**, a 4(1*H*)-pyridone with antiplasmodial activity, that inhibits mitochondrial respiration.[10] Introduction of a lipophilic side chain at C5 resulted in GW844520, **3**, which displays excellent in vitro activity against both blood and liver stages of *P. falciparum*.[10]

Virtual screening (VS) of chemically available ligand databases has become, in recent years, a useful tool to search chemical space and accelerate the initial stages of drug discovery. The technique can be based on the structure of the binding pocket or on the structure of known inhibitors. In either case the aim is to rapidly identify potential hit molecules, which can then be

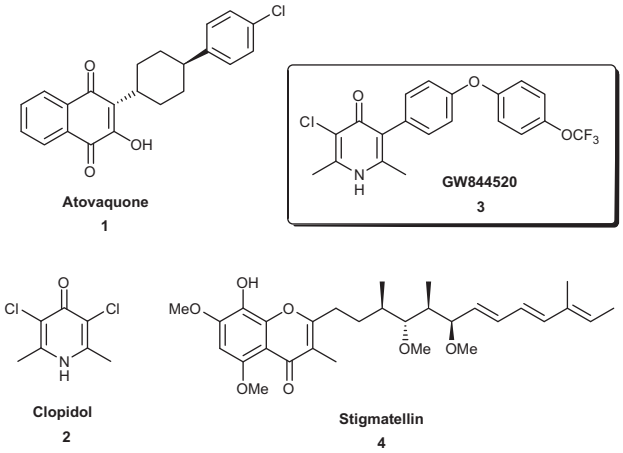

biologically evaluated. Despite the relatively high number of false positives inherently linked to this approach,[11–13] VS has recently been applied to tackle plasmodial drug targets such as

* Corresponding author. Tel.: +351 217946400; fax: +351 217946470.
E-mail address: rmoreira@ff.ul.pt (R. Moreira).

0968-0896/$ - see front matter © 2011 Elsevier Ltd. All rights reserved.
doi:10.1016/j.bmc.2011.09.004

falcipains,[14–16] dihydrofolate reductase,[17] spermidine synthase,[18] enoyl-acyl carrier protein reductase,[19] myosin tail interacting protein–myosin A complex[20] with encouraging results, as novel leads for optimization were discovered.

As part of our ongoing research regarding potential bc_1 complex inhibitors we set out to identify new leads with identical pharmacophoric features to GW844520 4(1*H*)-pyridone. Here we report the results of a VS study combining ligand- and structure-based approaches.

2. Results and discussion

2.1. Ligand-based virtual screening

With the intention of filtering out the two chemical databases (ZINC and MOE) in an expeditious way, a 3D pharmacophore model was generated using the MOE software, which is a highly regarded software for this purpose.[21,22] The model was generated from a possible bioactive pose of GW844520 obtained through docking at the Q_o site of the bc_1 complex (Fig. 1). The Q_o site is a highly convoluted pocket. Therefore, by understanding the pose of the 4(1*H*)-pyridone and using it to build a pharmacophore model, we expected to quickly discard many drug-like molecules that could not mimic the pose and did not have adequate distances between the key chemical features. In the present case, only GW844520 was used to build the pharmacophore model, given that:

(i) Currently there is a relative lack of chemotypes with potent activity against cytochrome bc_1;
(ii) The in vitro antiplasmodial assays were carried out against several different strains, making it difficult to compare potencies among different classes of compounds;
(iii) The inhibitors of the bc_1 complex may present different binding modes, making it inappropriate for aligning features, that is, the pharmacophores of the different classes of inhibitors bind distinctively to the active site;
(iv) The aim of the study was to find novel leads with similar pharmacophoric regions to the 4(1*H*)-pyridones.

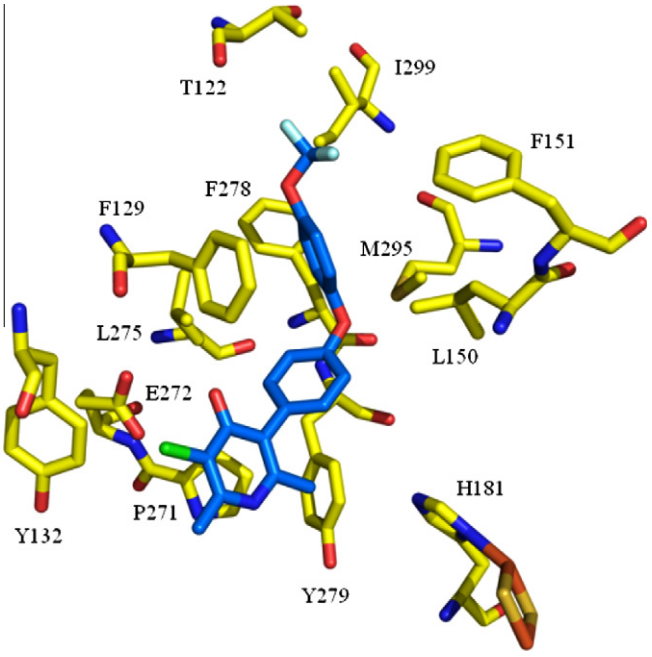

Figure 1. Docking pose of GW844520 in cytochrome bc_1.

GW844520 is one of the most potent cytochrome bc_1 inhibitors known to date (IC_{50} = 30 nM),[10] and to validate the generated model, a training set of fourteen 4(1*H*)-pyridones with structurally different substituents at either C3 and/or C5 was assembled. These were then subjected to a conformational sampling with MOE. Finally, the conformers were treated as rigid entities for the validation screening. The chemical structures and their IC_{50} values against the *P. falciparum* T9-96 strain[10] are given in Figure 2.

In MOE, a pharmacophore model consists of spheres depicting the tolerance zone allowed for each feature. The phamacophore model used for the ZINC drug-like database (model A)[23] consisted of seven features (Fig. 3A). Features F1 through F5 represent alternate hydrophobic and aromatic regions, with hydrophobic represented in green, that is, F1, F3 and F5, and aromatic in orange, that is, F2 and F4. The sphere radius was manually adjusted in order to optimize the model. Hence, F1 has a sphere radius 1.5 Å, F3 of 1.6 Å and F5 of 1.9 Å. The aromatic regions F2 and F4 have radii of 1.9 Å and 1.5 Å, respectively. Both hydrogen bond acceptor, F6, and donor, F7, have a radius of 1.0 Å.

Model A proved to be efficient in excluding compounds with an IC_{50} higher than 2,200 nM and compound **10**, with an IC_{50} of

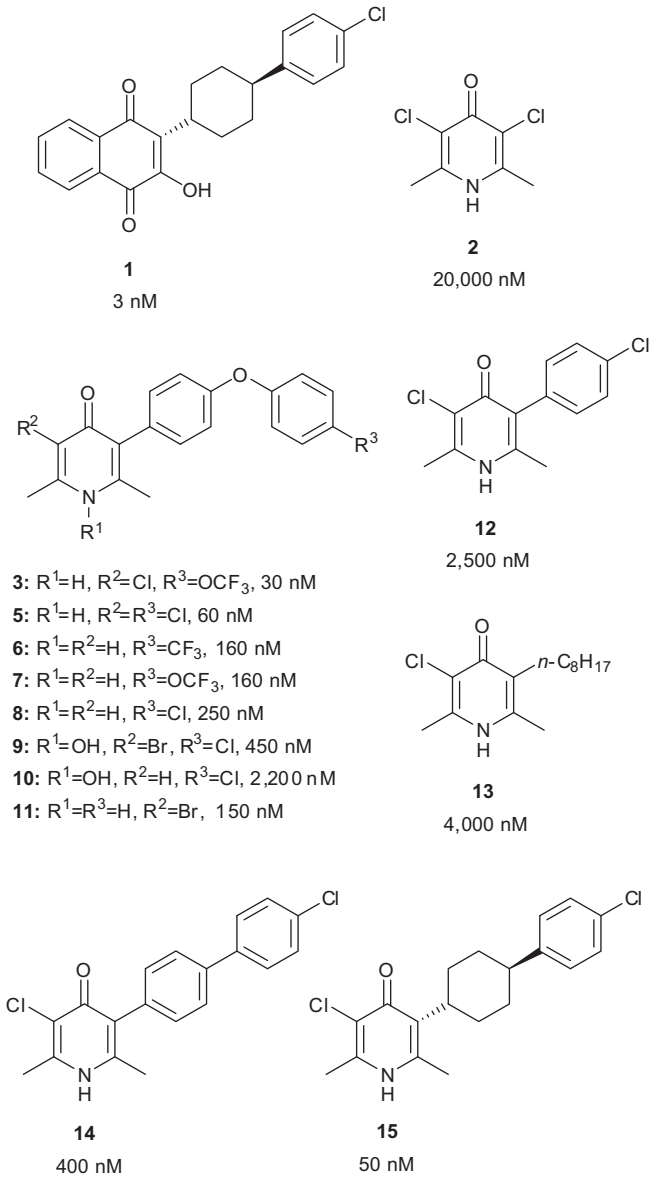

Figure 2. Structures and IC_{50}s of the training set.

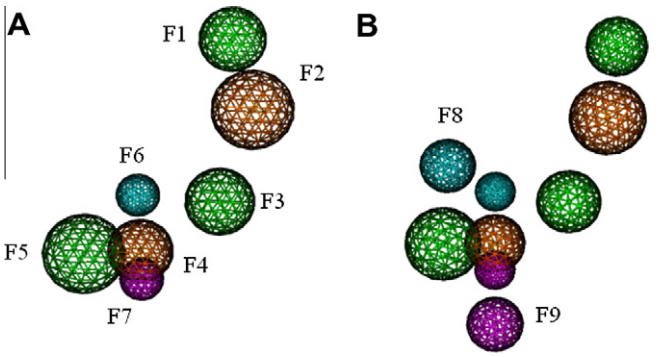

Figure 3. (A) Pharmacophore model used to screen the ZINC database; (B) Pharmacophore model used for the MOE database. Green spheres represent hydrophobic regions, orange represent aromatic regions, blue is a hydrogen-bond acceptor and its projection and purple represents a hydrogen-bond donor and its projection.

2,200 nM, presented the highest RMSD value amongst the 4(1*H*)-pyridones. Atovaquone presented the highest RMSD value of all hit molecules within the training set, despite its low IC_{50} against the T9-96 strain. Thus, the model is expected to be biased towards compounds presenting features related to those of the 4(1*H*)-pyridones, regardless of their bc_1 complex inhibitory potency.

Prior to executing the ligand-based VS, the ZINC database was filtered out with the Lipinski's rule of five.[24,25] Therefore, from roughly 8.5 million molecules, the database was reduced to *ca.* 0.5 million drug-like compounds. However, given that this was still a huge number of compounds to perform a conformational search, a second filter was applied —database clustering. The downloaded database consisted of 136,996 compounds, for which the conformational search was performed.

The in silico screen of the ZINC database was conducted with the pharmacophore model A. In this model, while features F4 and F5 correspond to the core pyridone scaffold, F1–F3 correspond to the critical hydrophobic side chain. 4(1*H*)-Pyridones with longer and mixed aromatic/hydrophobic features in the side chain, are markedly more active. Thus F1–F5 were deemed essential for a compound to be considered a hit. A partial match of six out of the seven features was allowed. This partial match permitted to drastically reduce the database size, while retaining pharmacophoric-related compounds without being excessively restrictive, that is, admitting compounds with the possibility of one hydrogen bond with either E272 or H181, like in stigmatellin, **4**. Around 1000 positive hits were obtained, according to this methodology (Fig. 4).

For the MOE drug-like database, over 600,000 compounds were supplied with the conformational library already constructed, and no other filters were applied before the VS. For this database screen, model A reduced the database size to *ca.* 10,000 molecules, which would be unsuitable for the structure-based VS stage. Therefore, a more restrictive model was built. Projections of both hydrogen bond acceptors and donors, F8 and F9, with a 1.4 Å radius, were added to the pharmacophore model A, resulting in model B (Fig. 3B). Similar results to those of model A were obtained in the validation screen. While screening the MOE database, no partial match was allowed, also due to the high number of hits when this setting was allowed for model B. Thus, employing this protocol, the size of the database was reduced to approximately 700 compounds that were selected for further refinement (Fig. 4).

2.2. Structure-based virtual screening

The hits were docked with GOLD software[26] into the cytochrome bc_1 model that had been validated in previous studies.[8,27] Given that structure-based VS can be computationally very

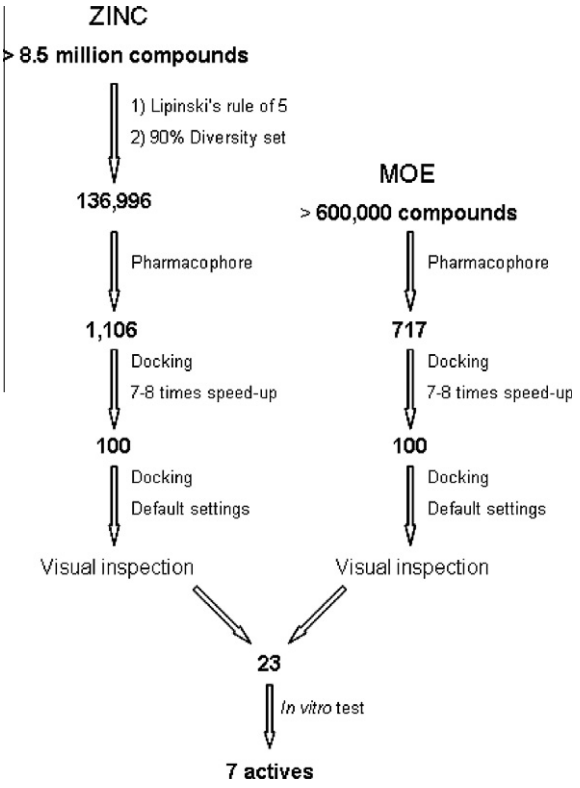

Figure 4. Virtual screening protocol breakdown.

demanding, it is relevant to find an approach that optimizes the balance between the precision of docking and the time required for the process. The initial stages of receptor-based virtual screening are generally executed to discard many compounds quickly. Exhaustive docking for the top ranked compounds can be carried out subsequently to estimate their binding pose and interactions with the receptor. Thus, in the present study, the docking processes were performed in three consecutive stages, employing different settings in GOLD. At first, VS was performed with 7–8 times speed-up settings. This is an optimized setting for VS protocols, since a lower number of genetic operations are done. As a result, a higher throughput is obtained, with acceptable accuracy rates in the prediction (60–70%).[26] The best 100 ligands of each database were subjected to further docking refinement, this time with standard settings, that is, a higher number of genetic operations, but a relatively low number of runs. This allowed a better prediction of the pose. While performing the screening with a higher number of genetic operations we noted significantly different poses from the ones obtained with speed-up settings, for some molecules. The final GoldScores were ordered, and each ligand was visually inspected for a similar docking pose to **3** and/or hydrogen bonding with H181 and E272. These two residues are involved in physiological electron transfer across the bc_1 complex and have been described to interact with Q_o site inhibitors.[7,8,27] For example, the carbonyl and the 5-OMe groups of stigmatellin are within hydrogen bonding distance of H181, while the 8-OH substituent is pointed towards E272.[28]

2.3. Antiplasmodial activity

From the 200 molecules visually inspected, 23 compounds were purchased (Fig. 5) and shifted to in vitro antiplasmodial testing against the *P. falciparum* W2 (chloroquine-resistant) strain. Out of the 23 compounds tested, 6 showed IC_{50}s in the 2–30 M range (Table 1).

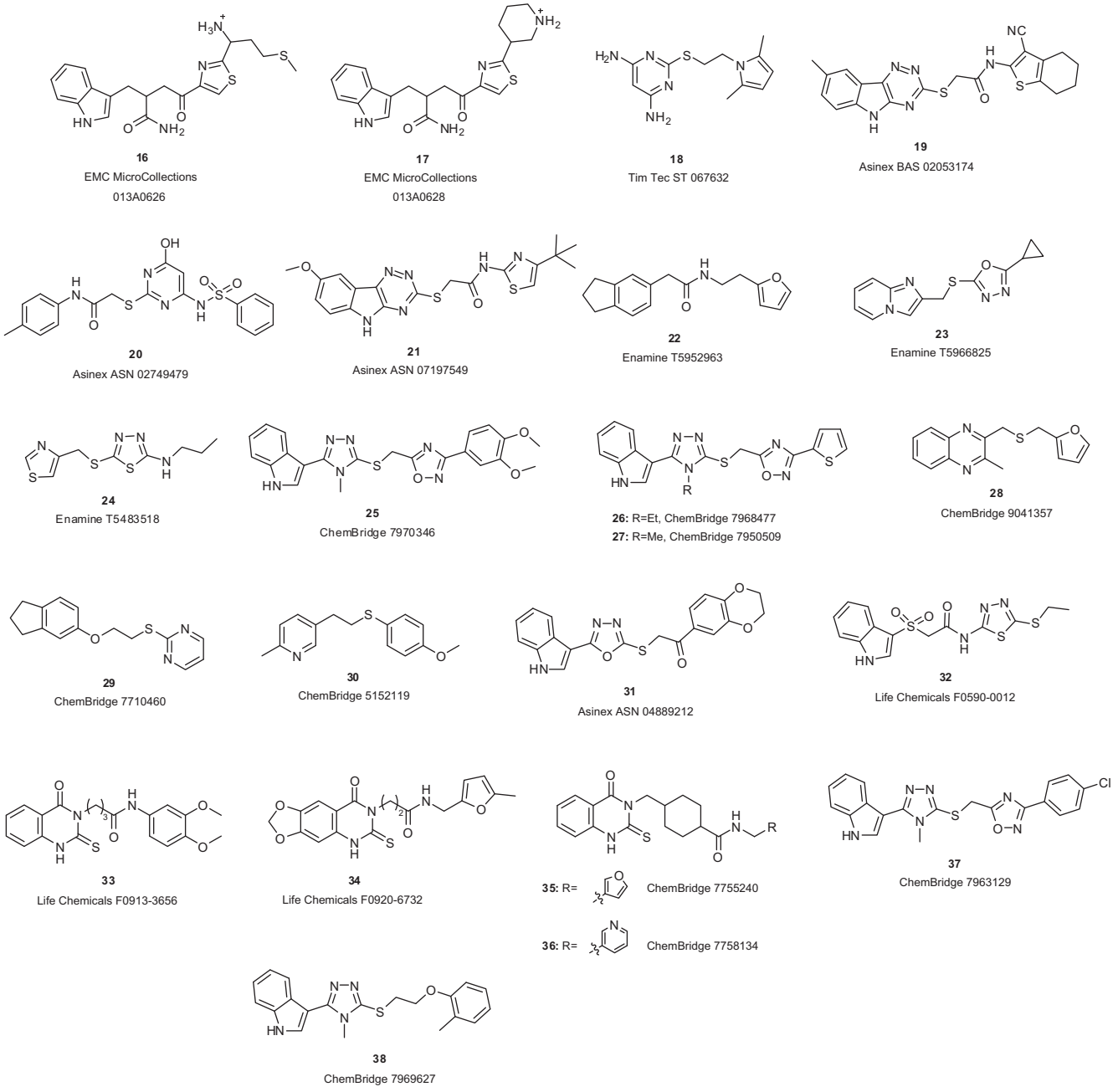

Figure 5. Structures of the compounds selected from the VS protocol.

Table 1
Antiplasmodial activity (W2 strain) for the selected compounds

Compd	IC_{50} ± SD (μM)	Compd	IC_{50} ± SD (μM)
16	>50	**28**	>50
17	>50	**29**	>50
18	>50	**30**	>50
19	>50	**31**	>50
20	>50	**32**	>50
21	27.1 ± 2.0	**33**	>50
22	>50	**34**	>50
23	>50	**35**	>50
24	>50	**36**	1.97 ± 0.9
25	12.1 ± 0.2	**37**	>50
26	28.5 ± 0.3	**38**	6.69 ± 2.1
27	29.5 ± 2.7		

Compounds **36** and **38** presented an IC_{50} below 10 μM, with the former displaying a value of 2 μM. While compound **25** exhibited activity with an IC_{50} value of 12 μM, most of the other active compounds presented IC_{50} values around 30 μM, that is, compounds **21**, **26** and **27**. All other compounds did not present noticeable activity up to the tested concentrations. These results are encouraging, and partly validate the virtual screening protocol, as it proved to be efficient in identifying active compounds within the top ranked ligands. The expected success rate for a good pharmacophore ranges from 0.5 to 20%, according to Shoichet et al.,[29] In this case, the overall success rate was 26% (6 out of 23). All of the active compounds were from MOE (44% success rate).

A third round of docking studies was performed to better predict the binding pose of the active compounds in the Q_o site. Taking

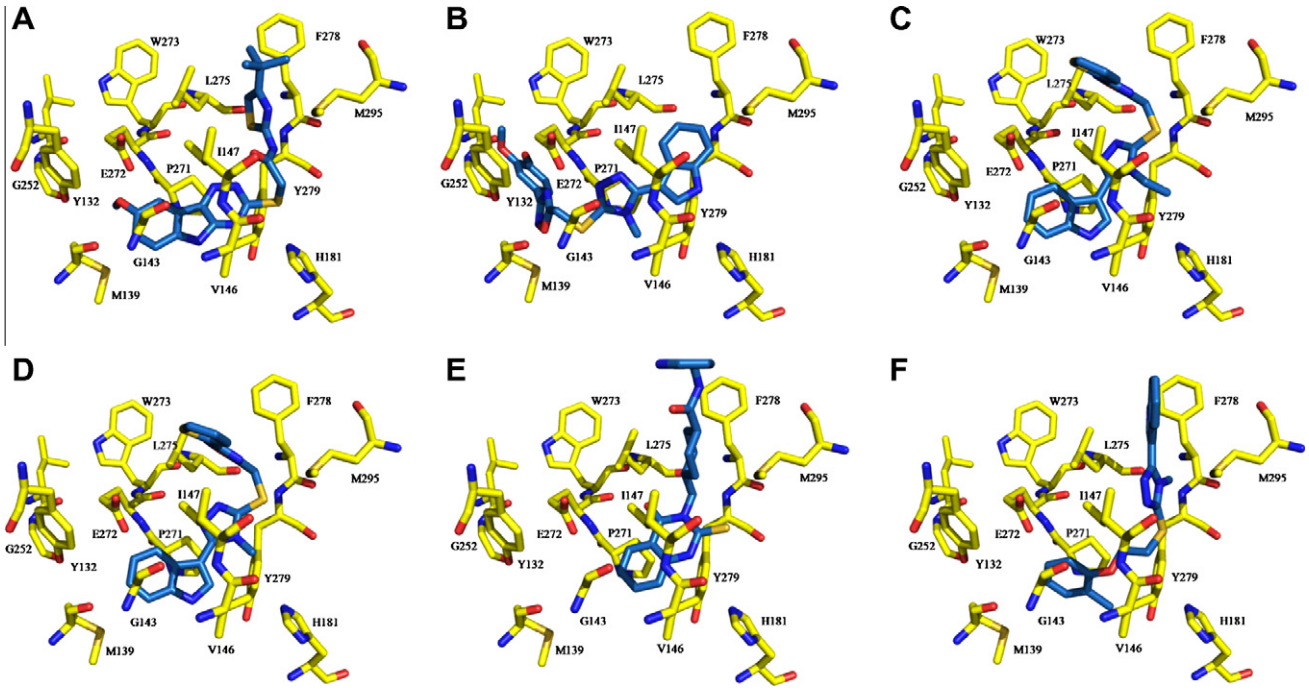

Figure 6. Docking poses of **21** (A); **25** (B); **26** (C); **27** (D); **36** (E); **38** (F).

the antiplasmodial activities and the docking poses together one can observe the following:

(i) The presence of a dimethoxyphenyl group in **25** is responsible for a twofold increase in activity when compared to its thiophene counterpart, that is, compound **27**. Moreover, the docking study reveals a different docking pose for **25** (Fig. 6B) to that of its related indole compounds **26** and **27** (Fig. 6C and D). The best docking poses for each of compounds **25–27** individualy were superimposable, indicating that the predictions are significantly different. This may help explain the different IC_{50} values, based on a stronger van der Waals interaction with the receptor, in the case of **25**. While the side chain is docked in proximity to the heme group for **25**, for **26** and **27** it is directed to the outer side of the binding pocket;

(ii) The insertion of an ethyl or methyl groups in the triazole moiety appears to be unimportant for antiplasmodial activity, that is, **26** versus. **27**;

(iii) Compound **38** displayed an analogous docking pose to **25**. Results were consistent with higher activity, for the triazolylindole subset of compounds. In this case, it appears that the oxadiazole ring in **25–27** is also detrimental for antiplasmodial activity. A more flexible linker to the terminal aryl moiety, for example, that in **38**, leaves the side chain better accommodated in the binding pocket;

(iv) Compound **36** displayed moderate antiplasmodial activity and a docking pose similar to **3**. The thioxo group was also within contact distance of H181;[30]

(v) Compound **35**, which differs only in the terminal aryl moiety from **36**, does not present an $IC_{50} \leqslant 50$ μM. Compound **35** exhibited a significantly different docking pose to that seen for **36**. Also, no superimposable docking pose to the one predicted for **36** was found within the top ranked poses of **35**. Altogether, this might explain the difference in IC_{50} values (ESI).

The active compounds present similar electronic distribution to the 4(1*H*)-pyridones. Also, the accordance of that distribution with the docking poses makes us believe that these compounds have the required features to inhibit the bc_1 complex. We are now in the process of optimizing the active compounds.

3. Conclusions

Several malarial drug targets have been virtually screened to identify novel leads for development. To the best of our knowledge, this is the first disclosure of new chemotypes resulting from a VS study targeting the bc_1 complex of malaria parasites. These results also highlight the successful combination of ligand- and structure-based virtual screening approaches to rapidly filter large databases with a high success rate. Scaffold hopping is one of the major goals in VS studies, particularly in ligand-based approaches. With this protocol, we were able to identify new leads for drug development in malaria, as no related analogs have been reported in the literature.

4. Experimental

4.1. Molecular docking

No crystal structure of the bc_1 complex from *Plasmodia* is available. Therefore, bc_1 complex from *Saccharomyces cerevisiae* (PDB code 1KYO)[31] was used, given there is a high sequence identity between the two species (~68%) within the Q_o binding pocket.[32] This presents the dimeric and functional protein with the iron–sulfur cluster in close contact with cytochrome *b*, which is crucial for electron transfer. The protein preparation was carried out using UCSF Chimera.[33] Hydrogens were added to aminoacid residues, partial charges were assigned with Antechamber,[34] the energy was minimized and the output saved as mol2 file. In 1KYO, histidine 181 at the Q_o site was kept protonated, as good evidence of this state is available for stigmatellin binding.[35] Docking was performed with the GOLD 4.01[26] package that searches for the best ligand interaction pose using a genetic algorithm. The docking model had previously been validated.[27] Docked ligands into the Q_o site were ranked with the GoldScore[36] scoring function. It in-

cludes the following components: protein-ligand hydrogen bond energy, protein-ligand van der Waals energy, ligand internal van der Waals energy and ligand torsional strain energy. This fitness function has been optimized to predict the ligand binding position and conformation of the ligands. Default settings were used and 10,000 docking runs were performed for each ligand.

4.2. Database filtration

The ZINC 8[23] database containing over 8.5 million compounds was used in this study. Database filtration was performed to collect only the drug-like compounds, by applying the Lipinski's rule of five.[25] A 90% diversity set (136,966 compounds) was submitted for VS. The database clustering was executed by analyzing similarities between the compounds. This was carried out with the algorithm of Bienfait, which incrementally selects compounds that differ from all previous considerations by the Tanimoto cutoff (90% diversity). This was readily available to download from ZINC. For the MOE 2008.10[21] database, only the drug-like subset, comprising over 600,000 compounds, was used.

4.3. Ligand-based virtual screening

The pharmacophore model was generated from the bioactive pose of GW844520, using the unified scheme in MOE. The algorithm uses active compounds to derive the pharmacophore without taking their biological data into account. Two different models were constructed and validated, including the following features: hydrophobic centroid, aromatic center, hydrogen-bond acceptor and its projection, hydrogen-bond donor and its projection. The radius of each feature was varied until a good selection of active molecules, within a training set of 14 compounds, was achieved. The training set resulted from the assembly of bc_1 complex inhibitors with a determined IC_{50} against the T9-96 *P. falciparum* strain. Importantly, we found a good correlation ($r^2 = 0.707$) between the root mean square deviation (RMSD) values and IC_{50}s of the 4(1*H*)-pyridones against the T9-96 strain of *P. falciparum*, which further validate the pharmacophoric models.[10] A conformational search using MOE was carried out to generate conformers for all compounds of the databases. In brief, this algorithm employs a parallelized fragment-based approach, in which molecules are divided into overlapping fragments. Each fragment is then submitted to a stochastic conformational search. The resulting fragment conformers are minimized and then assembled by superimposing common atoms. A maximum of 250 conformations/compound were generated, using the MMFF94x forcefield. A strain limit of 4 kcal/mol was employed, to limit redundant conformers. Virtual screening was then carried out for the two databases, and only the lowest RMSD result of each hit was saved.

4.4. Structure-based virtual screening

Structure-based virtual screening was performed with GOLD software. In the first stage of the screen, 500 runs on a 7–8 times speed up setting were conducted for each of the *ca.* 2000 compounds that matched the pharmacophore query. The top 100 results (~10%) from each database were selected for the second phase of the structure-based screen. This was performed with 250 runs under default settings. Only the top 5 poses of each compound were stored. This protocol helped to optimize the balance between the quality of the docking and the time required for the process. The results from the second phase of screening were visually inspected with PyMol[37], based on the following criteria: (i) hydrogen bond with H181 and E272; (ii) hydrophobic interactions and complementarity between ligand and binding pocket.

The active compounds from the in vitro tests were subjected to the third docking round. This consisted of 10,000 runs under default settings, in order to better predict the molecular interactions within the Q_o site of cytochrome bc_1.

4.5. In vitro screening

Human red blood cells infected with *P. falciparum* strain W2 at ~1% parasitemia, synchronized with 5% sorbitol, were incubated with test compounds in 96-well plates at 37 °C for 48 h, beginning at the ring stage, in RPMI-1640 medium, supplemented with 25 mM HEPES pH 7.4, 10% heat inactivated human serum (or 0.5% Albumax/2% human serum), and 100 μM Hypoxanthine, under an atmosphere of 3% O_2, 5% CO_2, 91% N_2. After 48 h the cells were fixed in 2% HCHO in PBS; transferred into PBS with 100 mM NH_4Cl, 0.1% Triton X-100, 1 nM YOYO-1; and analyzed in a flow cytometer (FACSort, Beckton Dickinson; EX 488 nm, EM 520 nm). IC_{50}s were calculated using GraphPad Prism software. All active compounds, with the exception of **21**, exhibited ⩾95% purity determined by the manufacturer using LC–MS and NMR.

Acknowledgments

The work was financially supported by Fundação para a Ciência e Tecnologia, through the doctoral grant SFRH/BD/30689/2006 (T.R.) and project PTDC/SAU-FCT/098734/2008. PJR is a Distinguished Clinical Scientist of the Doris Duke Charitable Foundation.

Supplementary data

Supplementary data associated with this article can be found, in the online version, at doi:10.1016/j.bmc.2011.09.004.

References and notes

1. WHO, World Malaria Report 2009.
2. Painter, H. J.; Morrisey, J. M.; Mather, M. W.; Vaidya, A. B. *Nature* **2007**, *446*, 88.
3. Kessl, J. J.; Meshnick, S. R.; Trumpower, B. L. *Trends Parasitol.* **2007**, *23*, 494.
4. Rodrigues, T.; Lopes, F.; Moreira, R. *Curr. Med. Chem.* **2010**, *17*, 929.
5. Looareesuwan, S.; Chulay, J. D.; Canfield, C. J.; Hutchinson, D. B. *Am. J. Trop. Med. Hyg.* **1999**, *60*, 533.
6. Fry, M.; Pudney, M. *Biochem. Pharmacol.* **1992**, *43*, 1545.
7. Kessl, J. J.; Lange, B. B.; Merbitz-Zahradnik, T.; Zwicker, K.; Hill, P.; Meunier, B.; Pálsdóttir, H.; Hunte, C.; Meshnick, S.; Trumpower, B. L. *J. Biol. Chem.* **2003**, *278*, 31312.
8. Rodrigues, T.; Santos, D. J. V. A. d.; Moreira, R.; Lopes, F.; Guedes, R. C. *Int. J. Quantum Chem.* **2011**, *111*, 1196.
9. Korsinczky, M.; Chen, N.; Kotecka, B.; Saul, A.; Rieckmann, K.; Cheng, Q. *Antimicrob. Agents Chemother.* **2000**, *44*, 2100.
10. Yeates, C. L.; Batchelor, J. F.; Capon, E. C.; Cheesman, N. J.; Fry, M.; Hudson, A. T.; Pudney, M.; Trimming, H.; Woolven, J.; Bueno, J. M.; Chicharro, J.; Fernández, E.; Fiandor, J. M.; Gargallo-Viola, D.; Heras, F. G.; Herreros, E.; León, M. L. *J. Med. Chem.* **2008**, *51*, 2845.
11. Eckert, H.; Bajorath, J. *Drug Discovery Today* **2007**, *12*, 225.
12. Klebe, G. *Drug Discovery Today* **2006**, *11*, 580.
13. Sun, H. *Curr. Med. Chem.* **2008**, *15*, 1018.
14. Desai, P. V.; Patny, A.; Sabnis, Y.; Tekwani, B.; Gut, J.; Rosenthal, P.; Srivastava, A.; Avery, M. *J. Med. Chem.* **2004**, *47*, 6609.
15. Desai, P. V.; Patny, A.; Gut, J.; Rosenthal, P. J.; Tekwani, B.; Srivastava, A.; Avery, M. *J. Med. Chem.* **2006**, *49*, 1576.
16. Li, H.; Huang, J.; Chen, L.; Liu, X.; Chen, T.; Zhu, J.; Lu, W.; Shen, X.; Li, J.; Hilgenfeld, R.; Jiang, H. *J. Med. Chem.* **2009**, *52*, 4936.
17. Adane, L.; Patel, D. S.; Bharatam, P. V. *Chem. Biol. Drug Des.* **2010**, *75*, 115.
18. Jacobsson, M.; Gäredal, M.; Schultz, J.; Karlén, A. *J. Med. Chem.* **2008**, *51*, 2777.
19. Nicola, G.; Smith, C. A.; Lucumi, E.; Kuo, M. R.; Karagyozov, L.; Fidock, D. A.; Sacchettini, J. C.; Abagyan, R. *Biochem. Biophys. Res. Commun.* **2007**, *358*, 686.
20. Kortagere, S.; Welsh, W. J.; Morrisey, J. M.; Daly, T.; Ejigiri, I.; Sinnis, P.; Vaidya, A. B.; Bergman, L. W. *J. Chem. Inf. Model.* **2010**, *50*, 840.
21. ChemicalComputingGroup *MOE: Molecular Operating Environment*, 2008.10; Montreal, 2008.
22. Wolber, G.; Seidel, T.; Bendix, F.; Langer, T. *Drug Discovery Today* **2008**, *13*, 23.
23. Irwin, J. J.; Shoichet, B. K. *J. Chem. Inf. Model.* **2005**, *45*, 177.
24. Lipinski, C. A.; Lombardo, F.; Dominy, B. W.; Feeney, P. J. *Adv. Drug Delivery Rev.* **1997**, *23*, 3.

25. Lipinski, C. A. *J. Pharmacol. Toxicol. Methods* **2000**, *44*, 235.
26. Jones, G.; Willett, P.; Glen, R. C. *J. Mol. Biol.* **1995**, *245*, 43.
27. Rodrigues, T.; Guedes, R. C.; dos Santos, D. J. V. A.; Carrasco, M.; Gut, J.; Rosenthal, P. J.; Moreira, R.; Lopes, F. *Bioorg. Med. Chem. Lett.* **2009**, *19*, 3476.
28. Hunte, C.; Koepke, J.; Lange, C.; Rossmanith, T.; Michel, H. *Structure* **2000**, *8*, 669.
29. Alvarez, J.; Soichet, B. In *Virtual Screening in Drug Discovery*; Taylor & Francis: Boca Raton, FL, 2005; p 451.
30. Bissantz, C.; Kuhn, B.; Stahl, M. *J. Med. Chem.* **2010**, *53*, 5061.
31. Lange, C.; Hunte, C. *Proc. Natl. Acad. Sci. U.S.A.* **2003**, *99*, 2800.
32. Kessl, J. J.; Ha, K. H.; Merritt, A. K.; Lange, B. B.; Hill, P.; Meunier, B.; Meshnick, S. R.; Trumpower, B. L. *J. Biol. Chem.* **2005**, *280*, 17142.
33. Pettersen, E. F.; Goddard, T. D.; Huang, C. C.; Couch, G. S.; Greenblatt, D. M.; Meng, E. C.; Ferrin, T. E. *J. Comput. Chem.* **2004**, *25*, 1605.
34. Wang, J.; Wang, W.; Kollman, P. A.; Case, D. A. *J. Mol. Graph. Model.* **2006**, *25*, 247.
35. Ritter, M.; Palsdottir, H.; Abe, M.; Mäntele, W.; Hunte, C.; Miyoshi, H.; Hellwig, P. *Biochemistry* **2004**, *43*, 8439.
36. Jones, G.; Willett, P.; Glen, R. C.; Leach, A. R.; Taylor, R. *J. Mol. Biol.* **1997**, *267*, 727.
37. DeLano, W. L. *The Pymol Molecular Graphics System*; DeLano Scientific: Palo Alto, CA, USA, 1997.